Size-controlled Synthesis of Gold Nanoparticles by Thermolysis of a Gold(I)-Sulfide Complex in the Presence of Alkylamines

Mari Yamamoto, Yukiyasu Kashiwagi, and Masami Nakamoto

Osaka Municipal Technical Research Institute, 6-50, 1-Chome, Morinomiya, Joto-ku,
Osaka 536-8553, Japan

Reprint requests to Dr. Masami Nakamoto. Fax: +81-6-6963-8099.
E-mail: nakamoto@omtri.city.osaka.jp

Dedicated to Professor Hubert Schmidbaur on the occasion of his 75th birthday

A size-controlled synthesis of gold nanoparticles has been developed by the thermolysis of AuCl(SMe$_2$) in the presence of alkylamines at 120 °C. In the procedure, the key intermediate was [Au(NH$_2$R)$_2$]Cl, detected by electrospray ionization (ESI) mass spectrometry. This thermally unstable intermediate was reduced by alkylamines under mild conditions to produce alkylamine-capped gold nanoparticles. The average diameters of the gold nanoparticles could be regulated in a range from 4.3 to 6.1 nm by applying primary alkylamines with alkyl chains of different lengths. Larger gold nanoparticles with diameters from 10 to 22 nm were prepared by a combination of alkylamines and alkylcarboxylic acids with various lengths of the alkyl chains. The gold nanoparticles were characterized by transmission electron microscopy (TEM), UV/Vis absorption spectroscopy, powder X-ray diffraction (PXRD), X-ray photoelectron spectroscopy (XPS), gas chromatography/mass spectroscopy (GC/MS), and thermogravimetric and differencial thermal analyses (TG/DTA).

Key words: Gold Nanoparticle, Controlled Thermolysis, Amine, Carboxylic Acid, Gold Complex

Introduction

The study of nanoparticles is generally motivated by the change in physical and chemical properties as compared to those of bulk materials. In particular, gold nanoparticles have been focused on because of their potential applications in electronics [1], optical devices [2], sensing [3,4], and catalysis [5]. Thus, the search for new preparation methods for gold nanoparticles has dramatically increased during the last decade [6]. A representative wet-chemical method was the reduction of a metal salt by a reducing agent in the presence of a stabilizer and a solvent. Brust *et al.* achieved the preparation of alkanethiol-capped gold nanoparticles by the two-phase reduction of HAuCl$_4$ using NaBH$_4$ as reducing agent [7]. Recently, amines have been employed as reducing agents for HAuCl$_4$ in synthesis protocols for gold nanoparticles. For example, *p-n*-hexadecylaniline in chloroform was used for the two-phase reduction of aqueous HAuCl$_4$ solutions, resulting in the formation of gold nanoparticles in the organic phase [8]. Some referential synthetic approaches are also based on the reduction of HAuCl$_4$ by fat-soluble oleylamine in water [9] or non-polar solvents [10]. As an alternative method, the thermolysis of gold(I) complexes has been developed. The benefit of this method is the control of the nanoparticle's growth rate by selection of the precursor and variation of its thermal stability, the stabilizer, and the reaction temperature and time. According to this synthetic approach, gold(I) complexes, such as Au(acac)PPh$_3$ [11] and [Au(μ-mesityl)]$_5$ [12] have been used as precursors. A time-dependent growth of gold nanoparticles has been observed during the thermolysis of Au(acac)PPh$_3$ in the presence of *n*-hexadecylamine (200 eq.) and tri-*n*-octylphosphine oxide (TOPO) (200 eq.) in diphenyl ether. The particle sizes of *n*-hexadecylamine- and TOPO-capped gold nanoparticles were controlled over a range from 10±1 nm to 50 nm with a larger size deviation in diameter [11]. The thermolysis of [Au(μ-mesityl)]$_5$ in the presence of *n*-octylamine (400 eq.) and TOPO (364 eq.) also afforded *n*-octylamine- and TOPO-capped gold nanoparticles with an average diameter of 12±1 nm [12]. The reduction of AuCl(amine) prepared from AuCl(tetrahydrothiophene) with *n*-octyl-

amine under 3 bars of H_2 for 15 h in THF solution in the presence of an excess of *n*-octylamine is one of the few examples using gold(I)-sulfide complexes. However, in this case the particle size could not be controlled to produce *n*-octylamine-capped gold nanoparticles with a broad size distribution [13].

In general, metal nanoparticles were prepared in diluted solutions in the presence of large amounts of stabilizer and solvent in order to prevent aggregation of the nanoparticles. In the case of the thermolysis of gold(I) complexes, *vide supra*, the preparation of gold nanoparticles was also performed in diluted solution [11, 12]. Contrary to the general method of particle synthesis, we have previously developed the thermolysis of gold(I) complexes $[RN(CH_3)_3][Au(SR)_2]$ in the presence of small amounts of alkylamines (1 eq.) without solvent to produce gold nanoparticles [14], and the growth of the gold nanoparticles could be controlled in the range form 7.5 to 23 nm in diameter, affording amine-, sulfide- and thiol-capped gold nanoparticles.

In this paper, we demonstrate the size-controlled synthesis of gold nanoparticles by the thermolysis of $AuCl(SMe_2)$ in the presence of primary alkylamines (NH_2R) and in the absence or presence of alkyl-carboxylic acids under concentrated conditions. The key reaction is the substitution of SMe_2 by an alkylamine. The intermediate $[Au(NH_2R)_2]Cl$ decomposes under mild heating to afford alkylamine-capped gold nanoparticles, and the released SMe_2 can be easily removed from the reaction solution due to its low boiling point of 38 °C. Considering the application of gold nanoparticles for electronics, the contamination of sulfur- and phosphine-derived capping ligands may corrode electronic circuits. However, GC/MS and XPS indicated no residual SMe_2 in the obtained alkylamine-capped gold nanoparticles. We have also systematically investigated the influence of the chain length of the employed alkylamines and alkylcarboxylic acids and their combinations on the particle size and the size distribution.

Results and Discussion

Synthesis and properties of gold nanoparticles, HDA-AuNP

Gold nanoparticles were prepared by the simple one-pot thermolysis of a gold(I)-sulfide complex in the presenc of an alkylamine. A representative synthesis of gold nanoparticles is the following. A mixture of $AuCl(SMe_2)$ [15] and *n*-hexadecylamine (HDA) was
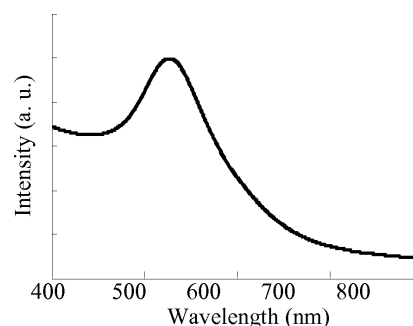

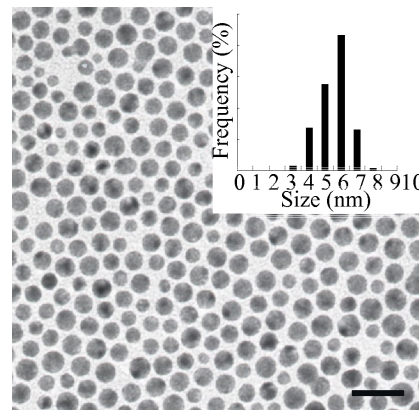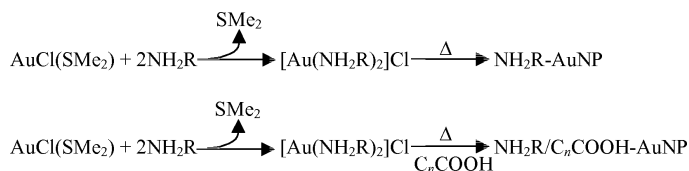Fig. 1. UV/Vis absorption spectrum of the amine-capped gold nanoparticles HDA-AuNP.

Fig. 2. TEM image (scale bar = 20 nm) of the amine-capped gold nanoparticles HDA-AuNP. The inset shows the corresponding size distribution.

heated to 120 °C for 1 h. The white suspension of $AuCl(SMe_2)$ in HDA gradually turned into a transparent and colorless solution at around 65 °C. Then, a gradual color change *via* red to purple occurred at 120 °C, indicating the formation of the gold nanoparticles [10]. The purification of the nanoparticles was accomplished by centrifugation in the mixed solvent acetone/methanol. The purified gold nanoparticles (HDA-AuNP) were isolated as a brown powder. The metal content of HDA-AuNP was 74 wt-%, the residual of 26 wt-% being the organic stabilizer, as determined by TG/DTA. The yield calculated by the weight and metal content of the isolated gold nanoparticles was 89 %. The HDA-AuNP particles could be re-dispersed in non-polar solvents such as toluene and *n*-hexane by ultrasonication, even after prolonged storage of the gold-nanoparticle powder in air. Furthermore, the re-dispersed solution showed no sign of precipitation of aggregates after one week. Fig. 1 shows the UV/Vis absorption spectrum of the re-dispersed HDA-AuNP in

$$AuCl(SMe_2) + 2NH_2R \xrightarrow{\text{SMe}_2} [Au(NH_2R)_2]Cl \xrightarrow{\Delta} NH_2R\text{-AuNP}$$

$$AuCl(SMe_2) + 2NH_2R \xrightarrow{\text{SMe}_2} [Au(NH_2R)_2]Cl \xrightarrow[C_nCOOH]{\Delta} NH_2R/C_nCOOH\text{-AuNP}$$

Scheme 1. Size-controlled synthesis of amine-capped gold nanoparticles by the thermolysis of $AuCl(SMe_2)$ in the presence of alkylamine (NH_2R) in the absence (top) and in the presence of alkylcarboxylic acid (C_nCOOH) (bottom).
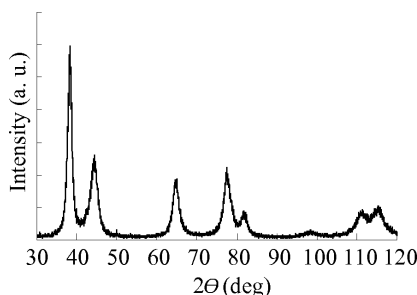

Fig. 3. PXRD pattern of the amine-capped gold nanoparticles HDA-AuNP.

toluene. The peak maximum was centered at 527 nm, which is the characteristic surface plasmon band for gold nanoparticles in toluene [10].

Fig. 2 shows a TEM image and the corresponding particle-size distribution of HDA-AuNP. The TEM sample was prepared using a toluene suspension of the nanoparticles directly without a size selection process. The average diameter and the standard deviation of HDA-AuNP based on the TEM image was 6.1 ± 0.9 nm. The HDA-AuNP particles were found to be spherical and nearly monodisperse. The crystal structure of HDA-AuNP was examined by powder X-ray diffraction (PXRD) (Fig. 3). The diffraction peaks at $2\theta = 38, 45, 65,$ and $78°$ could be indexed as the (111), (200), (220) and (311) planes of face-centered cubic gold, respectively. The line broadening of the PXRD peaks was primarily due to the smaller crystallite size [16]. The average crystallite size was calculated by the Scherrer equation [16] using the half width of the intense (111) reflection. The calculated average crystallite size of HDA-AuNP was 7.0 nm, corresponding with the value obtained from the TEM image of 6.1 ± 0.9 nm.

The XPS analyses indicates the binding energies for the Au $4f_{7/2}$ and Au $4f_{5/2}$ bands to be 84 and 87 eV, respectively (Fig. S1; see Supporting Information). These binding energies are in good agreement with those of zero-valent gold (Au $4f_{7/2}$: 84, Au $4f_{5/2}$: 88 eV) [17]. On the other hand, both Cl and S were not detected in HDA-AuNP (Fig. S2; see Supporting Information). The capping ligand of HDA-AuNP was

investigated by GC/MS analyses, proving the presence of HDA ($m/z = 241$), whereas SMe_2 was absent. Thus, only HDA is found to be attached to the surface of the gold core.

In the reaction process, the suspension of a white powder, $AuCl(SMe_2)$, in HDA gradually turned into a transparent and colorless solution at 65 °C. This phenomenon implies the formation of an intermediate derived from $AuCl(SMe_2)$ and HDA. In order to examine this intermediate, an ESI-MS experiment was carried out. A sample solution was prepared by refluxing a mixture of $AuCl(SMe_2)$ and an excess of HDA in THF for a few minutes. Fig. S3 (see Supporting Information) shows the ESI-MS spectrum measured in positive-ion mode. The peaks at $m/z = 679$ and 242 correspond to $[Au(HDA)_2]^+$ and RNH_3^+, respectively. Peaks corresponding to $[Au(SMe_2)]^+$, $[Au(SMe_2)(HDA)]^+$ and $[Au(HDA)]^+$ could not be detected. This result indicates that the intermediate is $[Au(HDA)_2]Cl$, derived from the substitution of SMe_2 by HDA. In addition, the released SMe_2 could be easily removed from the reaction solution as a vapor due to its low boiling point of 38 °C. In the reaction process, $AuCl(SMe_2)$ reacts with HDA to form the intermediate, $[Au(HDA)_2]Cl$, followed by the thermolysis of the intermediate to produce alkylamine-capped gold nanoparticles, as shown in Scheme 1 (top).

Particle size control by alkylamines with various chain lengths

We have previously demonstrated that the particle size and size distribution of gold nanoparticles can be controlled by the chain length of the alkylamines [14]. From this point of view, the gold nanoparticles were systematically prepared in the presence of primary alkylamines with different chain lengths, oleylamine (OLA) and *n*-dodecylamine (DDA). According to the preparation method of HDA-AuNP, the thermolysis of $AuCl(SMe_2)$ was carried out in the presence of OLA and DDA, respectively, at 120 °C for 1 h. Both types of gold nanoparticles, OLA-AuNP and DDA-AuNP, were quantitatively isolated as brown powders. Figs. 4a–c show TEM images and the corresponding particle-size
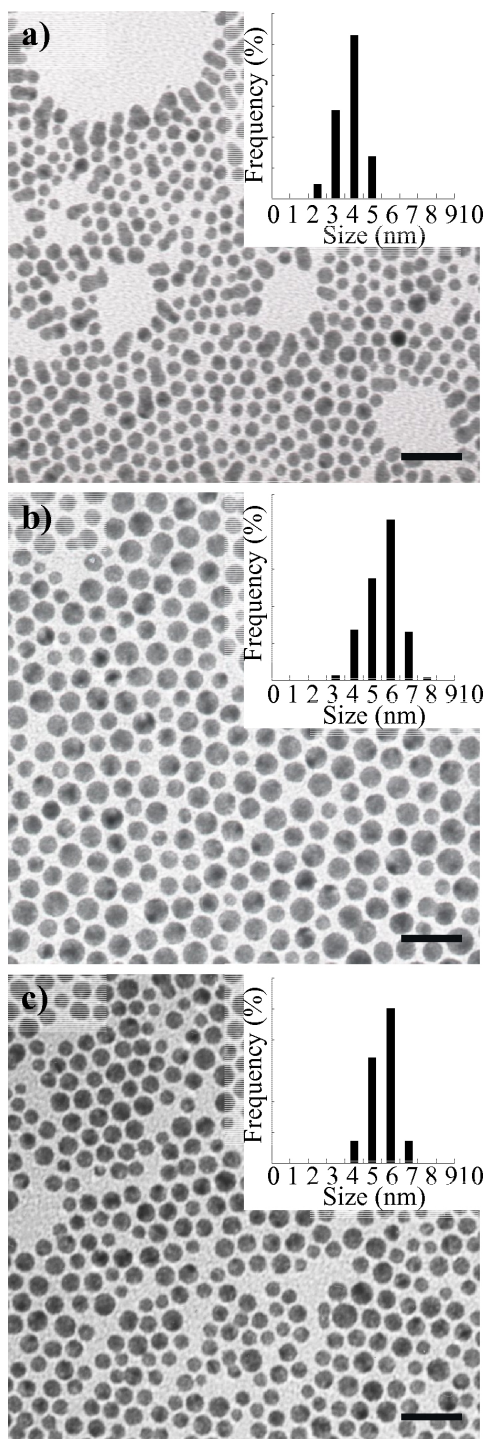
Fig. 4. TEM images (scale bar = 20 nm) of a series of amine-capped gold nanoparticles, a) OLA-AuNP, b) HDA-AuNP, and c) DDA-AuNP. The insets show their corresponding size distributions.

Table 1. Analytical data for gold nanoparticles NH_2R-AuNP (NH_2R = OLA, HDA, DDA).

| Nanoparticles	Capping ligand	Yield (%)	Diameter[a] (nm)
OLA-AuNP	OLA	99	4.3 ± 0.7
HDA-AuNP	HDA	89	6.1 ± 0.9
DDA-AuNP	DDA	95	6.1 ± 0.7

[a] TEM data.

distributions of OLA-AuNP, HDA-AuNP and DDA-AuNP, respectively. The yields and average diameters of the series of gold nanoparticles are summarized in Table 1. The average diameters and the standard deviations of OLA-AuNP, HDA-AuNP and DDA-AuNP based on TEM images are 4.3 ± 0.7 nm, 6.1 ± 0.9 nm and 6.1 ± 0.7 nm, respectively. The nanoparticles are spherical and nearly monodisperse. The growth of the core was well regulated to similar particle sizes by the alkylamines with various alkyl chain lengths in the range from C12 to C18. Compared with other gold nanoparticles prepared by the thermolysis of gold(I) complexes [11, 12, 14], the one in the present work have smaller particle sizes. Thus, primary alkylamines with a single long chain can effectively control the growth of the gold cores and thus afford relatively small nanoparticles. It is noticeable that the thermolysis of $AuCl(SMe_2)$ in the presence of branched alkylamines, such as 2-ethylhexylamine leads to an aggregation of the particles to generate bulk gold. The steric bulkiness of the branched alkylamines may hinder the coordination of the amine to the surface of the gold nanoparticles. Furthermore, the reaction of $AuCl(SMe_2)$ with tri-*n*-octylamine also produced bulk gold. Tertiary alkylamines are stronger reducing agents than primary alkylamines and are sterically more demanding compared to primary alkylamines. Therefore, the faster reduction of the gold(I) complexes and the weaker stabilization by the tertiary alkylamine promote the strong aggregation of the particles. These observations suggest that primary alkylamines with a straight long alkyl chain may strongly attach onto the surface of the nanoparticles through alkyl-alkyl interactions [18]. Thus, primary alkylamines with long alkyl chains are able to control the particle size and the size distribution more effectively than the branched and tertiary alkylamines.

Particle size control by alkylamines and alkylcarboxylic acids

The combination of alkylamines and alkylcarboxylic acids was widely used as stabilizer in the synthesis of alloy nanoparticles and metal-oxide nanopar-

Table 2. Analytical data for gold nanoparticles, NH_2R/C_nCOOH-AuNP (NH_2R = OLA, HDA; n = 13, 5).

Nanoparticles	Capping ligands	Yield (%)	Diameter[a] (nm)
OLA/C_{13}COOH-AuNP	OLA, C_{13}COOH	97	10 ± 1
OLA/C_5COOH-AuNP	OLA, C_5COOH	92	12 ± 1
HDA/C_{13}COOH-AuNP	HDA, C_{13}COOH	95	14 ± 1
HDA/C_5COOH-AuNP	HDA, C_5COOH	99	22 ± 5

[a] TEM data.
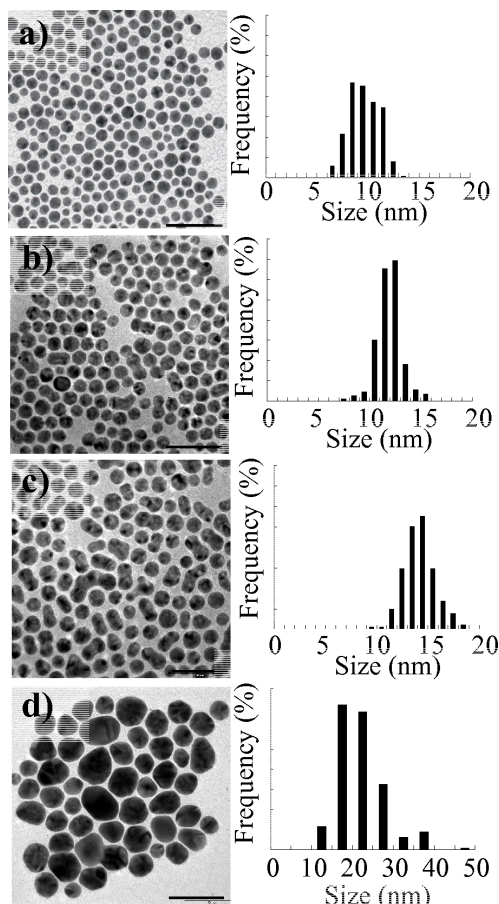
Fig. 5. TEM images (scale bar = 50 nm) and their corresponding size distributions of a series of amine/carboxylic acid-capped gold nanoparticles, a) OLA/C_{13}COOH-AuNP, b) OLA/C_5COOH-AuNP, c) HDA/C_{13}COOH-AuNP, and d) HDA/C_5COOH-AuNP.

ticles [19]. We have previously demonstrated that the particle size of silver nanoparticles can be controlled by the alkyl chain length of alkylamines and silver alkylcarboxylates [20–23]. For the purpose of size control of gold nanoparticles, alkylamines (OLA, HDA) and alkylcarboxylic acids, abbreviated as C_nCOOH (n = 13, 5), [n-tetradecanoic

acid (C_{13}COOH), n-hexanoic acid (C_5COOH)] were selected as capping ligands, as shown in Scheme 1 (bottom). In a representative procedure, $AuCl(SMe_2)$ was dissolved in alkylamine (NH_2R) at 65 °C to form [$Au(NH_2R)_2$]Cl. Then alkylcarboxylic acid was added to the reaction mixture, followed by heating at 100 °C for 1 h. The gold nanoparticles, NH_2R/C_nCOOH-AuNP (NH_2R = OLA, HDA; n = 13, 5), were isolated as brown powders. Figs. 5a–d show the TEM images and the corresponding size distribution of the gold nanoparticles OLA/C_{13}COOH-AuNP, OLA/C_5COOH-AuNP, HDA/C_{13}COOH-AuNP, and HDA/C_5COOH-AuNP, respectively. The yields and the average diameters of the series of NH_2R/C_nCOOH-AuNP are summarized in Table 2.

The average diameters and the standard deviations of OLA/C_{13}COOH-AuNP, OLA/C_5COOH-AuNP, HDA/C_{13}COOH-AuNP, and HDA/C_5COOH-AuNP based on TEM images are 10±1, 12±1, 14±1 and 22±5 nm, respectively. OLA/C_{13}COOH-AuNP, OLA/C_5COOH-AuNP and HDA/C_{13}COOH-AuNP are spherical and nearly monodisperse nanoparticles. However, in the case of HDA/C_{13}COOH-AuNP, some primary particles fused to each other to become peanut-shaped objects. This fusion of particles may be induced by the electron beam irradiation during TEM analyses. HDA/C_5COOH-AuNP revealed large and polydisperse nanoparticles with a distorted shape. Comparing OLA/C_{13}COOH-AuNP with OLA/C_5COOH-AuNP, the capping ligand with the longer alkylcarboxylic acid, C_{13}COOH, prevents the growth of gold cores. A similar trend in prarticle size was observed for HDA/C_{13}COOH-AuNP and HDA/C_5COOH-AuNP. A comparison of OLA/C_{13}COOH-AuNP with HDA/C_{13}COOH-AuNP revealed that OLA effectively prevents the growth and fusion of gold nanoparticles. Even though C_5COOH with its shorter alkyl chain was used as a capping ligand, the growth of OLA/C_5COOH-AuNP was prevented due to the stabilization by OLA. Thus, OLA functions are more effective as stabilizer for gold nanoparticles than HDA with its slightly shorter alkyl chain. The particles of NH_2R/C_nCOOH-AuNP are larger than the NH_2R-AuNP particles, as shown in Fig. 4. The gold core of NH_2R/C_nCOOH-AuNP is capped by both the alkylamine and the alkylcarboxylic acid. However, the stabilization of the soft gold core is effectively accomplished by alkylamine rather than by the hard alkylcarboxylic acid. Thus, weak adsorption of alkylcarboxylic acid promotes the growth of

NH$_2$R/C$_n$COOH-AuNP. Therefore, the growth of the gold core was systematically controlled by the chain length of the alkylamines and the alkylcarboxylic acids and their combination.

Conclusion

Size-controlled synthesis of almost monodisperse gold nanoparticles has been achieved by the thermolysis of AuCl(SMe$_2$) in the presence of alkylamines and in the absence or presence of alkylcarboxylic acids. The key intermediate, [Au(NH$_2$R)$_2$]Cl, detected by ESI-MS is likely to play the important role in producing almost monodisperse gold nanoparticles under the mild conditions of thermolysis. The average diameters of the gold nanoparticles could be controlled in a range from 4 to 22 nm by the combination of alkylamines and alkylcarboxylic acids and by variation of the alkyl chain lengths. This method gives reliably high yields of gold nanoparticles with a narrow size distribution. In addition, this method is applicable to industrial large-scale synthesis under concentrated conditions. The obtained gold nanoparticles did not show contamination by SMe$_2$, as demonstrated by XPS and GC/MS analyses. Furthermore, all the gold nanoparticles capped by alkylamines with or without alkylcarboxylic acids could be well dispersed in non-polar solvents. In essence, these new gold nanoparticles may be good candidates for nanoparticle inks applicable to printed electronics.

Experimental Section

Chemicals

All chemicals and solvents were of reagent grade quality, obtained commercially and used without further purification. HAuCl$_4$·4H$_2$O was purchased from Mitsuwa Chemicals Co., Ltd. Dimethylsulfide (SMe$_2$), oleylamine (OLA), *n*-hexadecylamine (HDA), *n*-dodecylamine (DDA), *n*-tetradecanoic acid (C$_{13}$COOH), *n*-hexanoic acid (C$_5$COOH), methanol, acetone, toluene, and THF were obtained from Nakarai Tesque, Inc. AuCl(SMe$_2$) was prepared according to the literature method [15].

Measurements

Thermogravimetric and differential thermal analyses (TG/DTA) were carried out on a Seiko Instruments SSC/5200 thermal analyzer. UV/Vis absorption spectra of nanoparticles re-dispersed in toluene were recorded on a Shimadzu UV-3150C spectrophotometer. The spectra were collected over a range of 300 – 800 nm. Transmission electron microscopic images were obtained on a JEM-1200EX transmission electron microscope (TEM) operated at 100 kV. Samples for TEM measurements were re-dispersed in toluene by ultrasonication and deposited on amorphous carbon film-coated copper grids followed by spontaneous evaporation at r. t. The average diameters and standard deviations of nanoparticles and particle size distributions were determined for more than 200 particles based on TEM images. Powder X-ray diffractions (PXRD) were measured using a Rigaku RINT 2500 diffractometer (monochromatized CuK_α radiation) operating at 40 kV and 50 mA. X-Ray photoelectron spectroscopy (XPS) was carried out on a Physical Electronics (PHI) model 5700 ESCA spectrometer with an Al monochromatic source (AlK_α energy of 1486.6 eV) using BN as the internal standard, and narrow scan photoelectron spectra were recorded for Au(4f), O(1s) and C(1s). Gas chromatography/mass spectroscopy (GC/MS) was carried out using a pyrolizer PY-2020D for thermal extraction at 200 °C for 10 min and a Hewlett-Packard 6890 GC system equipped with an HP 5973 mass-selective detector. ESI mass spectra (positive-ion mode) were obtained with an LCQ DECA mass spectrometer (ThermoQuest) and analyzed by the XCALIBER software on a Windows NT workstation. The measurement conditions were automatically optimized by tuning for the peak of the complex ion which was produced from a mixture of AuCl(SMe$_2$) and HDA in THF. The sample was infused using a syringe pump. The measurement conditions were as follows: spray voltage, 5.0 kV; spray current, 0.05 μA; sheath gas flow rate, 0.6 L min^{-1}; capillary voltage, 30 V; capillary temperature, 250 °C; syringe pump flow rate, 3 μL min^{-1}; mass range, *m/z* = 100 – 2000.

NH$_2$R-AuNP (NH$_2$R = OLA, HDA, DDA)

AuCl(SMe$_2$) (295 mg, 1.0 mmol) and the alkylamine (NH$_2$R = OLA, HDA or DDA) (10.0 mmol) were placed in a 10 mL flask equipped with a magnetic stirrer. The mixture was gradually heated to 120 °C. The mixture became transparent and colorless around 65 °C and turned into a homogeneous purple liquid at 120 °C. The mixture was heated for 1 h and then cooled to r. t. Acetone (5 mL) and methanol (1 mL) were added to the liquid to produce a suspension. The gold nanoparticles were collected by centrifugation at 2000 r. p. m. for 5 min, the solvents were decanted, and the residue was dried under vacuum. The gold nanoparticles (OLA-AuNP, HDA-AuNP, DDA-AuNP) prepared from alkylamines (NH$_2$R = OLA, HDA or DDA) were isolated as a brown powder, respectively.

NH$_2$R/C$_n$COOH-AuNP (NH$_2$R = OLA, HDA; n = 13, 5)

AuCl(SMe$_2$) (148 mg, 0.5 mmol) and alkylamine (NH$_2$R = OLA or HDA) (5.0 mmol) were placed in a 10 mL

flask equipped with a magnetic stirrer. After the suspension became a transparent and colorless liquid at 65 °C, alkylcarboxylic acid ($C_{13}COOH$ or C_5COOH) (5.0 mmol) was added to the solution. The mixture was gradually heated to 100 °C and kept for 1 h. The resulting purple solution was cooled to r. t., and acetone (5 mL) and methanol (1 mL) were added to the solution to precipitate the gold nanoparticles. They were collected by centrifugation at 2000 r. p. m. for 5 min, the solvents were decanted, and the residue was dried under vacuum. The gold nanoparticles (OLA/C_{13}COOH-AuNP, OLA/C_5COOH-AuNP, HDA/C_{13}COOH-AuNP and HDA/C_5COOH-AuNP) prepared from alkylamines (NH_2R = OLA, HDA) and alkylcarboxylic acids (C_{13}COOH, C_5COOH) were isolated as a brown powder.

[1] Y. Wu, Y. Li, P. Liu, S. Gardner, B. S. Ong, *Chem. Mater.* **2006**, *18*, 4627 – 4632.

[2] L. Tong, R. R. Gattass, J. B. Ashcom, S. He, J. Lou, M. Shen, I. Maxwell, E. Mazur, *Nature* **2003**, *426*, 816 – 819; M. Law, D. J. Sirbuly, J. C. Johnson, J. Goldberger, R. J. Saykally, P. Yang, *Science* **2004**, *305*, 1269 – 1273; Y. Nakayama, P. J. Pauzauskie, A. Radenovic, R. M. Onarato, R. J. Saykally, J. Liphardt, P. Yang, *Nature* **2007**, *447*, 1098 – 1102.

[3] M. Hu, J. Y. Chen, Z. Y. Li, L. Au, G. V. Hartland, X. D. Li, M. Marquez, Y. N. Xia, *Chem. Soc. Rev.* **2006**, *35*, 1084 – 1094.

[4] Y. Cui, Q. Wei, H. Park, C. M. Lieber, *Science* **2001**, *293*, 1289 – 1292.

[5] M. C. Daniel, D. Astruc, *Chem. Rev.* **2004**, *104*, 293 – 346; L. Yin, J. Liebscher, *Chem. Rev.* **2007**, *107*, 133 – 173.

[6] J. S. Bradley, G. Schmid in *Nanoparticles, From Theory to Application*, (Ed.: G. Schmid), Wiley-VCH, Weinheim, **2004**, chapter 3.2.1, pp. 186 – 199.

[7] M. Brust, M. Walker, D. Bethell, D. J. Schiffrin, R. Whyman, *J. Chem. Soc., Chem. Commun.* **1994**, 801 – 802.

[8] P. R. Selvakannan, S. Mandal, R. Pasricha, S. D. Adyanthaya, M. Sastry, *Chem. Commun.* **2002**, 1334 – 1335.

[9] M. Aslam, L. Fu, M. Su, K. Vijayamohanan, V. P. Dravid, *J. Mater. Chem.* **2004**, *14*, 1795 – 1797.

[10] H. Hiramatsu, F. E. Osterloh, *Chem. Mater.* **2004**, *16*, 2509 – 2511.

[11] D. A. Fleming, M. E. Williams, *Langmuir* **2004**, *20*, 3021 – 3023.

[12] S. D. Bunge, T. J. Boyle, T. J. Headley, *Nano Lett.* **2003**, *3*, 901 – 905.

[13] S. Gomez, K. Philippot, V. Colliere, B. Chaudret, F. Senocq, P. Lecante, *Chem. Commun.* **2000**, 1945 – 1946.

[14] M. Nakamoto, Y. Kashiwagi, M. Yamamoto, *Inorg. Chim. Acta* **2005**, *358*, 4229 – 4236.

[15] F. Bonati, G. Minghetti, *Gazz. Chim. Ital.* **1973**, *103*, 373.

[16] P. Scherrer, *Göttinger Nachrichten* **1918**, *2*, 98.

[17] D. I. Nichols, A. S. Charleston, *J. Chem. Soc. (A)* **1969**, 2581.

[18] A. Ulman in *An Introduction to Ultrathin Organic Films*, Academic Press, San Diego, **1991**; A. Ulman, *Chem. Rev.* **1996**, *96*, 1533.

[19] D. V. Talapin, E. V. Shevchenko, H. Weller, in *Nanoparticles, From Theory to Application*, (Ed.: G. Schmid), Wiley-VCH, Weinheim, **2004**, chapter 3.2.2.2, pp. 202 – 219.

[20] M. Yamamoto, M. Nakamoto, *J. Mater. Chem.* **2003**, *13*, 2064 – 2065.

[21] M. Yamamoto, Y. Kashiwagi, M. Nakamoto, *Langmuir* **2006**, *22*, 8581 – 8586.

[22] Y. Kashiwagi, M. Yamamoto, M. Nakamoto, *J. Colloid Interface Sci.* **2006**, *300*, 169 – 175.

[23] M. Nakamoto, M. Yamamoto, Y. Kashiwagi in *Metal Nanoclusters in Catalysis and Materials Science, The Issue of Size Control*, (Eds.: B. Corain, G. Schmid, N. Toshima), Elsevier, Amsterdam, **2008**, chapter 24, pp. 367 – 372.